AGU PUBLICATIONS

JGR

Journal of Geophysical Research: Oceans

RESEARCH ARTICLE

10.1002/2016JC012377

Vertically varying Eulerian mean currents induced by internal coastal Kelvin waves

Jan Erik H. Weber[1]

[1]Department of Geosciences, University of Oslo, Oslo, Norway

Key Points:
- The horizontal Eulerian mean current exhibits a Poiseuille type behavior
- The Eulerian current is stronger than the Stokes drift in Van Mijenfjorden

Correspondence to:
J. E. H. Weber,
j.e.weber@geo.uio.no

Citation:
Weber, J. E. H. (2017), Vertically varying Eulerian mean currents induced by internal coastal Kelvin waves, *J. Geophys. Res. Oceans*, *122*, 1222–1231, doi:10.1002/2016JC012377.

Received 27 SEP 2016
Accepted 24 JAN 2017
Accepted article online 31 JAN 2017
Published online 15 FEB 2017

Abstract The lost momentum in spatially damped internal Kelvin waves reappears as Eulerian mean currents through the action of the nonlinear wave-wave interaction terms. A novel expression is derived for the steady balance between the frictional force on the coastally trapped horizontal Eulerian mean flow, and the forcing from the wavefield in terms of the mean wave Reynolds stresses and the horizontal divergence of the Stokes drift. The forcing can be expressed in terms of orthogonal eigenfunctions for internal waves, yielding the vertical variation of the Eulerian mean flow. For arbitrary values of the Brunt-Väisälä frequency N, it is shown that the wave forcing on the Eulerian mean is always negative, yielding a Poiseuille type flow. Therefore, unlike the Stokes drift velocity in internal Kelvin waves which exhibits a backward drift for the first mode in the region of maximum N, the wave-induced horizontal Eulerian mean current is always in the direction of the waves. The results are illustrated by an example from Van Mijenfjorden in Svalbard, which is an arctic sill fjord where internal waves are generated by the action of the barotropic semidiurnal tide.

1. Introduction

Csanady [1972] was apparently the first to suggest that the mean flow associated with internal Kelvin waves may have a significant impact on the transport of nearshore effluents in lakes. Motivated by this, *Wunsch* [1973] derived the solution for an internal Kelvin wave forced by wind stress. He then calculated the Stokes drift of this wave, assuming that the Eulerian drift contribution was negligible. His results indicated that the drift in internal Kelvin waves may explain certain observed circulation patterns in lakes. *Ou and Bennett* [1979] argued that the Stokes drift itself was not observable by conventional current meters, and that the Eulerian mean should be included in the derivations to second order in wave amplitude. They studied a hypothetical circular lake, where the applied forcing was a horizontally uniform, diurnally oscillating wind stress. *Ou and Bennett* claimed that the resulting drift pattern may explain observed circulation patterns in Lake Kinneret, Israel.

As pointed out by *Wunsch*, a variable wind stress can excite internal Kelvin waves. But also tidal forcing is important in this connection. For example, in layered systems with strong barotropic tidal flow over bottom sills, we may find pronounced internal waves, e.g., *Farmer and Smith* [1980]. In Arctic regions, with ice cover for a long period of the year, the barotropic tide will constitute the main generating mechanism for internal waves. Along the Siberian Shelf and in the Canadian Archipelago, we find considerable internal wave activity due to tidal forcing [see e.g., *Levine*, 1990; *Morozov and Pisarev*, 2002, 2003; *Morozov et al*., 2003, 2008].

Since the Stokes drift associated with Kelvin waves in a continuously stratified fluid is well described in the literature [*Wunsch*, 1973; *Weber et al*., 2014; *Weber and Ghaffari*, 2014], the main focus of the present study is the wave-induced Eulerian mean current. As pointed out for two-layer models by *Ou and Bennett* [1979] and *Støylen and Weber* [2010], this current depends on the effect of friction on the waves as well as on the mean flow. We here consider the case of continuous stratification, writing the vertical part of the linear wave solutions in terms of orthogonal eigenfunctions for arbitrary values of the Brunt-Väisälä frequency [see e.g., *Gill and Clarke*, 1974]. The nonlinear forcing of the Eulerian mean current can then be expressed in terms of these functions, yielding the vertical variation of this flow. The rest of this paper is organized as follows: in section 2, we state the basic assumptions and the governing equations, and in section 3, we consider spatially damped linear wave motion. Here the details have been deferred to Appendix A. Section 4 presents the Stokes drift in terms of the eigenfunctions for the linear problem, while section 5 discusses the wave-induced Eulerian mean velocity with emphasis on its vertical variation. In section 6, the theory is

applied to Van Mijenfjorden in Svalbard, arctic Norway. Finally, section 7 contains a short discussion and some concluding remarks.

2. Basic Assumptions and Governing Equations

We consider a semi-infinite viscous ocean of constant depth H, bounded laterally by a straight coast. We chose a Cartesian coordinate system (x, y, z) such that the origin is situated at the undisturbed surface, the x axis is directed along the coast, and the y axis is positive toward the sea with the coast at $y=0$. The z axis is directed vertically upward, and the respective unit vectors are $(\vec{i}, \vec{j}, \vec{k})$. The reference system rotates about the vertical axis with angular velocity $f/2$, where f is the constant Coriolis parameter. Furthermore, we use an Eulerian description of motion, which means that all dependent variables are functions of x, y, z and time t. We take that the horizontal scale of the motion is so large compared to the depth that we can make the hydrostatic approximation in the vertical. Furthermore, we apply the Boussinesq approximation for the density ρ. We also take that the density of an individual fluid particle is conserved. The governing equations for this problem then become

$$\frac{\partial \vec{v}_h}{\partial t} + \vec{v} \cdot \nabla \vec{v}_h = -f\vec{k} \times \vec{v}_h - \frac{1}{\rho_r} \nabla_h p + \nu_T \frac{\partial^2 \vec{v}_h}{\partial z^2}, \tag{1}$$

$$\frac{\partial p}{\partial z} = -\rho g, \tag{2}$$

$$\frac{\partial \rho}{\partial t} + \vec{v} \cdot \nabla \rho = 0, \tag{3}$$

$$\nabla \cdot \vec{v} = 0. \tag{4}$$

Here $\vec{v} = (u, v, w)$ is the velocity vector, p is the pressure, subscript h means horizontal values, ρ_r is a constant reference density, and g the acceleration due to gravity. A simple eddy formulation has been assumed for the effect of friction, where ν_T is a constant eddy coefficient for the diffusion of momentum. Furthermore, we have assumed that the vertical variation of the turbulent stresses is much larger than the corresponding horizontal variation.

In the future analysis, we separate the variables into mean quantities (marked by an over-bar) and periodic wave components with zero mean (marked by a tilde).

3. Linear Internal Coastal Kelvin Waves

We consider coastally trapped internal waves propagating in the x direction. The waves result from small perturbations from a state of rest characterized by a horizontally uniform stable stratification $\rho_0(z)$. We take that the velocity in the y direction vanishes identically ($\tilde{v}=0$), characterizing the Kelvin wave. Introducing the vertical displacement $\xi(x, y, z, t)$ of the isopycnals from their original horizontal position, linear theory yields $\partial\tilde{\xi}/\partial t = \tilde{w}$, where the tilde is used to denote linear time-periodic perturbation quantities. The linear theory is trivial, and well described in the literature. For didactic reasons we have deferred some details to Appendix A. However, we state the linear equations here, since they are needed when we later on calculate the wave-wave interaction terms. We obtainfrom (1) to (4):

$$\begin{aligned}
\frac{\partial \tilde{u}}{\partial t} &= -\frac{1}{\rho_r}\frac{\partial \tilde{p}}{\partial x} + \nu_T \frac{\partial^2 \tilde{u}}{\partial z^2}, \\
f\tilde{u} &= -\frac{1}{\rho_r}\frac{\partial \tilde{p}}{\partial y}, \\
\frac{\partial \tilde{p}}{\partial z} &= -\rho_r N^2 \tilde{\xi}, \\
\tilde{\rho} &= \frac{\rho_r}{g} N^2 \tilde{\xi} \\
\frac{\partial \tilde{u}}{\partial x} &= -\frac{\partial^2 \tilde{\xi}}{\partial z \partial t}.
\end{aligned} \tag{5}$$

Here N is the Brunt-Väisälä frequency defined by

$$N^2 = -\frac{g}{\rho_r}\frac{d\rho_0(z)}{dz}. \tag{6}$$

The variables may be separated into normal modes [*Lighthill*, 1969], and we refer to *Gill and Clarke* [1974] for details; see also Appendix A.

4. The Stokes Drift

For historic reasons we first recapitulate the Stokes drift in internal waves. As first shown by *Stokes* [1847], periodic waves possess nonzero mean wave momentum, leading to a net drift of particles in the fluid. This mean drift is referred to as the Stokes drift, and is basically related to the inviscid part of the wavefield, eventually modified by a slow temporal or spatial viscous decay of wave amplitude. To second order in wave steepness the Stokes drift $\bar{u}_S$ in the x direction can be expressed by the Eulerian wavefield [*Longuet-Higgins*, 1953]:

$$\bar{u}_S = \overline{(\int \tilde{u}dt)\partial\tilde{u}/\partial x} + \overline{(\int \tilde{v}dt)\partial\tilde{u}/\partial y} + \overline{(\int \tilde{w}dt)\partial\tilde{u}/\partial z}, \tag{7}$$

where the over-bar denotes average over one wave period $T = 2\pi/\omega$. In the present problem we have $\tilde{v} = 0$, $\tilde{w} = \partial\tilde{\xi}/\partial t$, and $\partial\tilde{u}/\partial x = -\partial^2\tilde{\xi}/\partial t\partial z$. Hence, from (7) for internal Kelvin waves:

$$\bar{u}_S = \frac{\partial}{\partial z}\left(\overline{\tilde{u}\tilde{\xi}}\right). \tag{8}$$

By inserting from (A4):

$$\bar{u}_S = \sum_{n=1}^{\infty}\frac{c_n A_n^2}{2}\left[(\phi_n')^2 + \phi_n\phi_n''\right]\exp\left(-2\alpha_n x - 2y/a_n\right). \tag{9}$$

The expression (9) is valid for arbitrary $N(z)$. We write

$$\bar{u}_S = \sum_{n=1}^{\infty}\bar{u}_{Sn}(z)\,\exp\left(-2\alpha_n x - 2y/a_n\right). \tag{10}$$

Substituting from (A2), and defining $Z = z/H$, we obtain that

$$\bar{u}_{Sn} = B_n\left[\left(\frac{d\phi_n}{dZ}\right)^2 - \frac{H^2N^2}{c_n^2}\phi_n^2(Z)\right], \tag{11}$$

where B_n is the Stokes velocity scale given by

$$B_n = \frac{c_n A_n^2}{2H^2}. \tag{12}$$

Since the second term in (11) is always negative, we realize that the Stokes drift component for the mode in question must be negative at the z-level where the horizontal wave velocity is zero. This was first shown by *Wunsch* [1973] for baroclinic Kelvin waves in the case of constant Brunt-Väisälä frequency. In fact, by integration in the vertical, and application of the boundary conditions $\tilde{\xi} = 0$ for $z = -H,\ 0$ for baroclinic flow; see (A3), we find from (8) for the Stokes volume flux in internal coastal Kelvin waves that

$$\bar{U}_S = \int_{-H}^{0}\bar{u}_S dz = 0, \tag{13}$$

see also *Weber et al*. [2014] for internal equatorial Kelvin waves.

5. Equations for the Eulerian Mean Velocity

The mean horizontal Lagrangian (particle) velocity can generally be written as a sum of the Stokes drift velocity $(\bar{u}_S, \bar{v}_S)$ and an Eulerian mean current $(\bar{u}_E, \bar{v}_E)$ [*Longuet-Higgins*, 1953]. Like the Stokes drift, we

derive the Eulerian mean current to second order in wave steepness. We here consider steady motion. Utilizing the fact that $\tilde{v}=0$ for this problem, we find from (1) and (4) for the Eulerian mean second order variables:

$$\begin{aligned} -f\bar{v}_E &= -\frac{1}{\rho_r}\frac{\partial \bar{p}}{\partial x} - \frac{\partial(\overline{\tilde{u}\tilde{u}})}{\partial x} - \frac{\partial(\overline{\tilde{w}\tilde{u}})}{\partial z} + \nu_T \frac{\partial^2 \bar{u}_E}{\partial z^2}, \\ f\bar{u}_E &= -\frac{1}{\rho_r}\frac{\partial \bar{p}}{\partial y} + \nu_T \frac{\partial^2 \bar{v}_E}{\partial z^2}, \\ \frac{\partial \bar{w}_E}{\partial z} &= -\frac{\partial \bar{u}_E}{\partial x} - \frac{\partial \bar{v}_E}{\partial y}. \end{aligned} \tag{14}$$

Note that even though $\tilde{v}=0$ for the linear Kelvin wave, the mean velocity $\bar{v}_E$ in the y direction will be nonzero (but small), as we show later. Finally, $\bar{w}_E$ is a small vertical Eulerian mean velocity due to the nonzero horizontal divergence.

The conservation of density (3) yields to the same order, utilizing that $\tilde{\rho}=\rho_r N^2\tilde{\xi}/g$:

$$N^2\bar{w}_E = \frac{\partial(N^2\overline{\tilde{u}\tilde{\xi}})}{\partial x} + \frac{\partial(N^2\overline{\tilde{\xi}\partial\tilde{\xi}/\partial t})}{\partial z}. \tag{15}$$

We realize from (A4) that the last term on the right-hand side is identically zero. Hence, if $N^2(z)\neq 0$, we have for the vertical mean velocity

$$\bar{w}_E = \frac{\partial(\overline{\tilde{u}\tilde{\xi}})}{\partial x}, \tag{16}$$

representing the wave-induced mean upwelling. Interestingly, by combining (8) and (16), we obtain the novel result:

$$\frac{\partial \bar{w}_E}{\partial z} = \frac{\partial \bar{u}_S}{\partial x}, \tag{17}$$

relating the upwelling to the divergence of the Stokes drift. This is an extension of *Weber et al.* [2014], where it was shown that $\bar{w}_E=0$ for undamped internal waves (i.e., when $\partial\bar{u}_S/\partial x=0$).

By taking the curl of (14), and assuming that $|\partial\bar{v}_E/\partial x| \ll |\partial\bar{u}_E/\partial y|$ (to be verified later), we obtain

$$-f\frac{\partial \bar{w}_E}{\partial z} = \frac{\partial^2}{\partial x\partial y}(\overline{\tilde{u}\tilde{u}}) + \frac{\partial^2}{\partial y\partial z}\left(\overline{\tilde{u}\partial\tilde{\xi}/\partial t}\right) - \nu_T\frac{\partial^3 \bar{u}_E}{\partial y\partial z^2}. \tag{18}$$

By utilizing (17):

$$\nu_T\frac{\partial^3 \bar{u}_E}{\partial y\partial z^2} = \left[\frac{\partial^2}{\partial x\partial y}(\overline{\tilde{u}\tilde{u}}) + \frac{\partial^2}{\partial y\partial z}\left(\overline{\tilde{u}\partial\tilde{\xi}/\partial t}\right) + f\frac{\partial \bar{u}_S}{\partial x}\right]. \tag{19}$$

Assuming a coastally trapped solution, i.e., $\bar{u}_E \to 0$, when $y\to\infty$, and noticing that all the terms on the right-hand side are proportional to $\exp(-2\alpha_n x - 2y/a_n)$, we find from (19):

$$\nu_T\frac{\partial^2 \bar{u}_E}{\partial z^2} = \left[\frac{\partial}{\partial x}(\overline{\tilde{u}\tilde{u}}) + \frac{\partial}{\partial z}\left(\overline{\tilde{u}\partial\tilde{\xi}/\partial t}\right) + f\frac{\partial}{\partial x}\int \bar{u}_S dy\right]. \tag{20}$$

This equation, which appears to be new, expresses the steady balance in the fluid between the frictional force on the mean flow and the forcing from the wavefield. On the right-hand side the first two terms represent the action of the mean wave Reynolds stresses. The last term is particularly interesting. It originates from the combination of the vertical mean vorticity and the conservation of mean density in a rotating stratified fluid. The result is proportional to the horizontal divergence of the Stokes drift; see (17). The solution of (20) can be written

$$\bar{u}_E = \sum_{n=1}\bar{u}_{En}(z)\exp(-2\alpha_n x - 2y/a_n). \tag{21}$$

Inserting from (A4) and (9), utilizing that $fa_n=c_n$, we find

$$\nu_T \frac{d^2\bar{u}_{En}}{dz^2} = -\alpha_n A_n^2 N^2(z)\phi_n^2(z). \tag{22}$$

The right-hand side here is negative for all z. The solution to this equation yields a flow in the positive x direction, which is similar to what we find for pressure driven viscous flow in channels or pipes (Poiseuille flow).

We write the Brunt-Väisälä frequency as $N^2(z)=N_0^2F(z)$, where N_0 denotes the maximum value of N. From (A5) we recall that $\alpha_n/\nu_T=\hat{N}^2/(2c_n^3)$. Introducing the dimensionless height scale $Z=z/H$, we can write (22)

$$\frac{d^2\bar{u}_{En}}{dZ^2} = -\frac{H^2\hat{N}^2N_0^2A_n^2}{2c_n^3}F(Z)\phi_n^2(Z). \tag{23}$$

Assuming a free-slip condition at the surface (no external forcing), i.e., $d\bar{u}_{En}/dZ=0$ at $Z=0$, and a no-slip condition at the bottom, $\bar{u}_{En}(Z=-1)=0$, the solution is quite simply

$$\bar{u}_{En}(Z) = \frac{H^2\hat{N}^2N_0^2A_n^2}{2c_n^3}\int_{-1}^{Z} G(q)dq, \tag{24}$$

where

$$G(q) = \int_q^0 F(Z)\phi_n^2(Z)dZ. \tag{25}$$

For constant N, i.e., $N=N_0$, and $F=1$, the normalized eigenmodes are $\phi_n=\sin(n\pi Z)/n\pi$. Hence, from (24):

$$\bar{u}_{En} = \frac{H^2N_0^4A_n^2}{8n^2\pi^2c_n^3}\left(1-Z^2+\frac{1}{2n^2\pi^2}[1-\cos(2n\pi Z)]\right), \tag{26}$$

demonstrating that the Eulerian mean current is always positive above the bottom. In the next section we specify $N^2(Z)$ for a given location (Van Mijenfjorden in Svalbard). Then we solve (23) numerically.

Again, we emphasize that the Eulerian mean current derived here is caused by the mean momentum loss from the wavefield due to friction. In a steady state, there is a balance between this forcing from the waves and the action of bulk friction on the Eulerian mean flow; see (20). In *Wunsch* [1973], the effect of friction was not taken into account. Then α_n in (22) is identically zero, and there is no forcing from the waves. Accordingly, the Eulerian mean current vanishes, as pointed out by Wunsch.

The offshore Eulerian mean velocity is obtained from the continuity equation in (14), using (17):

$$\frac{\partial\bar{v}_E}{\partial y} = -\frac{\partial\bar{u}_E}{\partial x} - \frac{\partial\bar{w}_E}{\partial z} = -\frac{\partial}{\partial x}(\bar{u}_E+\bar{u}_S). \tag{27}$$

We note that the right-hand side represents the horizontal divergence of the alongshore Lagrangian mean velocity. Applying the boundary condition $\bar{v}_E=0$ at $y=0$, we find that

$$\bar{v}_E = \sum_{n=1}\alpha_n a_n(\bar{u}_{En}+\bar{u}_{Sn})[1-\exp(-2y/a_n)]\exp(-2\alpha_n x). \tag{28}$$

Since $\alpha_n a_n$ is a small quantity, we realize that $|\bar{v}_E| \ll |\bar{u}_E|, |\bar{u}_S|$. This justifies the assumption $|\partial\bar{v}_E/\partial x| \ll |\partial\bar{u}_E/\partial y|$ in the vorticity equation (18). The result (28) implies a small flux of mass into the region outside the coastally trapped zone. We return to this flux in the discussion of the mean horizontal circulation in sections 6 and 7.

From (16) we finally obtain for the wave-induced upwelling velocity:

$$\bar{w}_E = \sum_{n=1}\bar{w}_{En}\exp(-2\alpha_n x - 2y/a_n). \tag{29}$$

Here

$$\bar{w}_{En} = -\frac{\nu_T \hat{N}^2 A_n^2}{2c_n^2}\phi_n(z)\frac{d\phi_n}{dz}, \tag{30}$$

where we have utilized (A5). We note that $\bar{w}_E$ satisfies the boundary conditions at the surface and at the bottom for any value of $N^2(z)$, since $\phi_n(0)=\phi_n(-H)=0$ in this problem. Ideally, in ice-covered sill fjords this upwelling could be of importance, but as shown in the example in the next section, the upwelling velocities due to damped internal waves are very small.

6. Application to Van Mijenfjorden

Van Mijenfjorden is a 50 km long sill fjord at the west coast of Spitsbergen. The mean width of the fjord is about 10 km (see Figure 1). The island Akseløya lies across the mouth of the fjord, leaving two narrow sounds where the exchange between the fjord and the outside waters takes place. The sounds north and south of Akseløya, Akselsundet, and Mariasundet, both exhibit considerable tidal currents. The current is especially strong in Akselsundet, where numerical models and drifter experiments yield velocities of 2–3 m s^{-1} [*Kowalik et al*., 2015]. In the present paper, we do not consider the complicated flow in the vicinity of the sills, but focus on the internal wave motion in the stratified fjord induced by the semidiurnal tidal pumping [*Støylen and Weber*, 2010; *Skarđhamar and Svendsen*, 2010; *Støylen and Fer*, 2014]. Although it is evident that periodic internal waves occur in Van Mijenfjorden, it should be pointed out that we cannot exclude the possibility that some of the variability in this fjord may be due to internal solitary waves [see e.g., *Vlasenko et al*., 2005], or nonlinear wave packets [*Grimshaw and Helfrich*, 2012]. However, a discussion of the mean drift in solitary waves is outside the scope of the present paper.

We intend to apply our previous results obtained for a vertical coastal wall and a flat bottom to the real Van Mijenfjorden. Obviously, we then have to make some compromises. Since the wave motion basically occurs within one Rossby radius (here: 4–5 km) from the coast, and the displacement amplitude has its maximum at the coastal wall, the effective depth H in our model is less than the maximum depth in the fjord. To cover both the outer and the inner (more shallow) basin, we take that $H=60$ m in our analysis.

Støylen and Weber [2010] modeled the density distribution under the ice-covered Van Mijenfjorden as a two-layer system. In the summer season, when the fjord is ice free, the density distribution is far from a two-layer structure [see e.g., *Skarđhamar and Svendsen*, 2010, their Figure 3]. Measurements in July–August show variations of the vertical distribution of salinity and temperature in the surface layer due to varying wind conditions. But basically, the increasing salinity is reasonably well modeled by a hyperbolic tangent. We take for the salinity variation during summer conditions that

$$S = S_0 + S_1 \tanh(-bz/H), \tag{31}$$

where $S_0=25$ psu, $S_1=9$ psu, and $b=4$. In cold polar waters, the density change due to small temperature variations can be neglected. Furthermore, we assume that the density varies linearly with respect to the salinity. The expansion coefficient β due to salt is taken to be $\beta=8\times10^{-4}$ psu^{-1}. Then the summer (model) Brunt-Väisälä frequency N in the Van Mijenfjorden is obtained from

$$N^2 = -\frac{g}{\rho_r}\frac{d\rho_0}{dz} = N_0^2 F(Z), \tag{32}$$

where

$$N_0^2 = \frac{gb\beta S_1}{H}, \quad F(Z) = 1/\cosh^2(-bZ). \tag{33}$$

The graph of N^2 is displayed in Figure 2. The eigenvalue problem (A2) and (A3) is easily solved by a simple shooting procedure. The various baroclinic modes are readily obtained, but we assume that most of the wave energy resides in the first mode [*Lighthill*, 1969]. We therefore concentrate on this mode for the rest of this analysis.

Utilizing (32), we obtain numerically for the phase speed and the Rossby radius for first baroclinic mode that

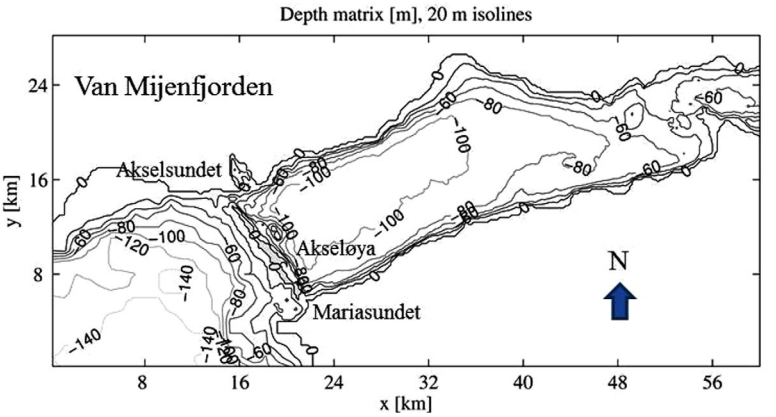

Figure 1. Coastline and bottom topography in Van Mijenfjorden in Svalbard, situated at 77.8°N, 15.5°E. Akseløya is displayed in gray.

$$c_1 = 0.59 \text{ m s}^{-1}, \qquad a_1 = c_1/f = 4.9 \text{ km}. \tag{34}$$

Earlier estimates from two-layer models for the baroclinic phase speed are $c_1 = 0.6\,\text{m s}^{-1}$ [*Skarđhamar and Svendsen*, 2010], and $c_1 = 0.55\,\text{m s}^{-1}$ [*Støylen and Weber*, 2010] which fit well with the first mode (34) for continuous stratification. Utilizing that the semidiurnal barotropic tidal forcing M_2 at the sill has a period of 12.4 h, the wavelength λ_1 of the first baroclinic mode becomes 26.2 km.

Scaling the Stokes drift for the first mode by

$$B_1 = \frac{c_1 A_1^2}{2H^2}, \tag{35}$$

we obtain from (11) that

$$\bar{u}_{S1} = B_1 \left[\left(\frac{d\phi_1}{dZ} \right)^2 - \frac{H^2 N^2}{c_1^2} \phi_1^2 \right]. \tag{36}$$

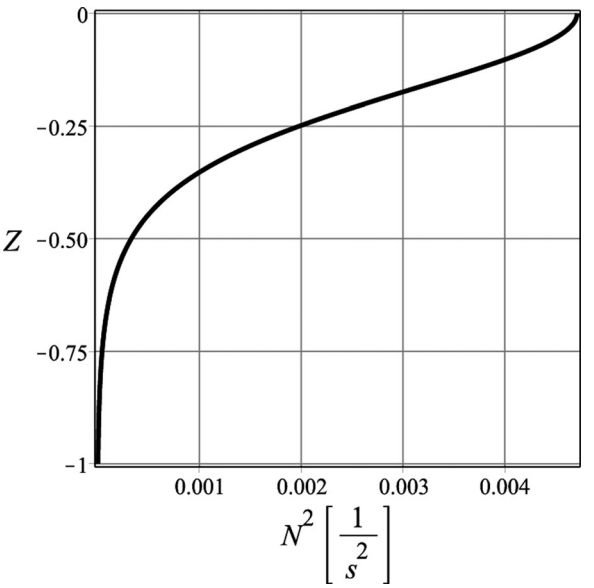

Figure 2. Idealized N^2 as function of nondimensional depth $Z = z/H$ for summer conditions in Van Mijenfjorden.

From the numerical results for $\phi_1(Z)$, the Z-dependence of the nondimensional Stokes drift $u_S = \bar{u}_{S1}/B_1$ is plotted in Figure 3. An earlier study of the Stokes drift in Van Mijenfjorden [*Støylen and Weber*, 2010] applied a two-layer model. This configuration produced positive Stokes drifts in both layers (negligible in the deep lower layer), and failed to yield the negative Stokes drift as found in the pycnocline for the first baroclinic mode (see Figure 3).

The Eulerian mean velocity for the first mode is obtained numerically from (23), with $F(Z) = 1/\cosh^2(-bZ)$ from (33), again with free-slip at the surface and no-slip at the bottom. The result, scaled with (35), is plotted in Figure 4. We note that the Eulerian mean current increases monotonically with height, with a maximum at the surface.

For the bulk value of the stratification used in the friction term (A5), we take $\hat{N}^2 = 2\times$

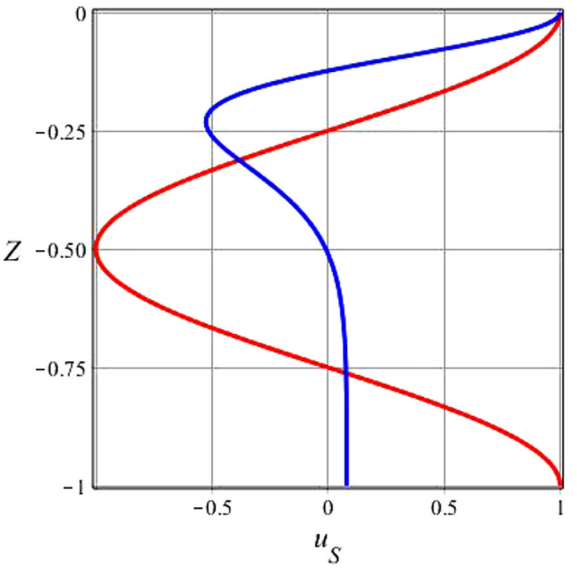

Figure 3. The nondimensional Stokes drift $u_S = \bar{u}_{S1}/B_1$ for the first Kelvin mode versus nondimensional depth Z (blue curve). The red curve is the corresponding Stokes drift obtained for constant Brunt-Väisälä frequency [see e.g., *Wunsch*, 1973].

$10^{-3}\,s^{-2}$ which is a fairly average value (see Figure 2). A typical value for the amplitude of the first baroclinic mode in Van Mijenfjorden near the right-hand shore is about 10 m. This order of magnitude is consistent with the observations of *Skardhamar and Svendsen* [2010] and *Støylen and Fer* [2014]. Hence, we take $A_1 = 10\,m$ in our analysis. From (35), we then obtain that $B_1 = 0.815\,\mathrm{cm\,s^{-1}}$. The maximum wave-induced Lagrangian drift velocity at the surface then becomes from our calculations (see Figures 3 and 4):

$$\bar{u}_{L1} = \bar{u}_{S1} + \bar{u}_{E1} = (1.0 + 2.64) \times B_1 = 3\,\mathrm{cm\,s^{-1}}. \tag{37}$$

In Figure 5, we have displayed the dimensional Stokes drift and the Eulerian mean velocity variation with depth. We note that the Eulerian mean velocity dominates in the entire water column. In Figures 3–5, we have only displayed the z-dependence of the drift currents. For a practical discussion, it is important to include the exponential decay from the coast within the internal Rossby radius as well as the weak exponential decay along the coast.

In this example, the maximum cross-shore surface velocity for the first mode at the outer edge of the trapping region $(y > a_1)$, is obtained from (28). It becomes $\bar{v}_{E1} = \alpha_1 a_1 \bar{u}_{L1}$, where $\bar{u}_{L1}$ is given by (37). A middle-of-the-road value for the eddy viscosity in van Mijenfjorden is assessed to be $\nu_T = 10^{-3}\,\mathrm{m^2 s^{-1}}$ [*Støylen and Weber*, 2010]. Hence, with $a_1 = 4.9\,\mathrm{km}$ from (34), we find that $\bar{v}_{E1} = 0.02\,\bar{u}_{L1} = 0.06\,\mathrm{cm\,s^{-1}}$ at the surface. The small cross-shore mean velocity decreases with depth, yielding a positive volume flux into the interior fjord basin.

The upwelling velocity from (30) is even smaller. We note the change in sign of the upwelling where the first mode horizontal wave velocity has its zero crossing. For the same parameters as before: $c_1 = 0.59\,\mathrm{m\,s^{-1}}$, $A_1 = 10\,\mathrm{m}$, and $\nu_T = 10^{-3}\,\mathrm{m^2\,s^{-1}}$, $\hat{N}^2 = 2 \times 10^{-3}\,\mathrm{s^{-2}}$, we find that the maximum upwelling velocity is about $3 \times 10^{-5}\,\mathrm{cm\,s^{-1}}$. Accordingly, wave-induced upwelling is probably negligible compared to the effect of turbulent diapycnal mixing in Van Mijenfjorden.

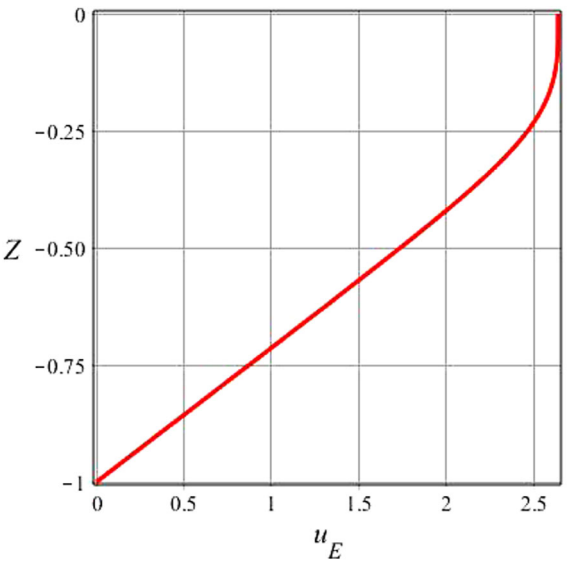

Figure 4. The nondimensional Eulerian mean current $u_E = \bar{u}_{E1}/B_1$ for the first Kelvin mode versus nondimensional depth Z.

7. Discussion and Concluding Remarks

The Lagrangian drift velocity induced by spatially damped internal coastal Kelvin waves is parallel to the coast, and trapped within the internal Rossby radius. For the first baroclinic mode in the ice-free Van Mijenfjorden, the Eulerian mean drift velocity is significantly larger than the Stokes drift, and is at all depths directed in the wave propagation direction. The alongshore mass transport associated with the Lagrangian mean drift $\bar{u}_L = (\bar{u}_{S1} + \bar{u}_{E1})\,\exp(-2\alpha_1 x - 2y/a_1)$, and the

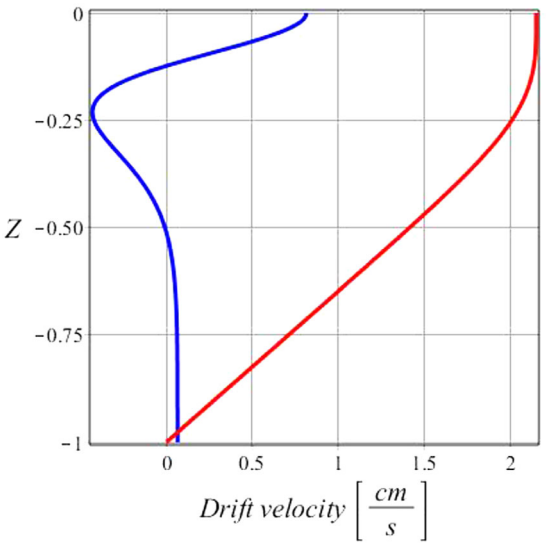

Figure 5. The dimensional Stokes drift $\bar{u}_{S1}$ (blue curve) and the dimensional Eulerian mean velocity $\bar{u}_{E1}$ (red curve) versus nondimensional depth.

offshore transport related to $\bar{v}_E$ in (28) will ultimately lead to mass accumulation in the interior of the fjord causing a geostrophic return flow; see the numerical results by *Støylen and Weber* [2010] for a two-layer model. Hence, the regular generation of internal Kelvin waves by action of the semidiurnal barotropic tide at the sills of Van Mijenfjorden is likely to produce a cyclonic horizontal mean circulation in the fjord. This circulation will be superimposed on the flow driven directly by the barotropic tide itself [see *Kowalik et al.*, 2015].

As far as the wave-induced circulation in Van Mijenfjorden is concerned, we do not think that the presence of an ice cover matters very much. In an ice-covered fjord a somewhat different density stratification will modify the eigenfunctions, without changing the Stokes drift very much. For the Eulerian mean current, it would be natural to suppose a no-slip condition at the contact with the ice. This would cause a current maximum below the surface (the ice). But the tidal pumping will keep up the turbulent eddy activity in the fjord, and hence the wave damping, so major changes of the magnitude of the Eulerian mean current is not expected.

Appendix A: Linear Internal Coastal Kelvin Waves

According to the adopted approach, we assume that

$$\left.\begin{aligned} \tilde{u} &= \sum_{n=1}^{\infty} u_n(x,y,t)\,\phi'_n(z), \\ \tilde{v} &= 0, \\ \tilde{p} &= \rho_r \sum_{n=1}^{\infty} p_n(x,y,t)\,\phi'_n(z), \\ \tilde{\xi} &= \sum_{n=1}^{\infty} \xi_n(x,y,t)\,\phi_n(z), \end{aligned}\right\} \tag{A1}$$

where the primes denote differentiation with respect to z. Separation of variables requires that $p_n = c_n^2 \xi_n$, where c_n is the constant eigenvalue. The eigenfunctions ϕ_n are solutions of

$$\phi''_n + \frac{N^2}{c_n^2}\phi_n = 0. \tag{A2}$$

For the baroclinic modes we assume a rigid lid at the surface [see *Gill and Clarke*, 1974]. Hence, the boundary conditions become

$$\phi_n = 0, \quad z = -H,\ 0. \tag{A3}$$

Letting real parts represent the physical solution, we find for spatially damped waves:

$$\begin{aligned} \xi_n &= A_n \exp(-\alpha_n x - y/a_n)\cos(k_n x + l_n y - \omega t), \\ u_n &= c_n A_n \exp(-\alpha_n x - y/a_n)\left[\cos(k_n x + l_n y - \omega t) + \frac{\alpha_n}{k_n}\sin(k_n x + l_n y - \omega t)\right], \end{aligned} \tag{A4}$$

where ω is a prescribed wave frequency. The wave number k_n and the small spatial attenuation coefficient α_n in the x direction become, respectively

$$k_n = \frac{\omega}{c_n}, \quad \alpha_n = \frac{\nu_T \hat{N}^2}{2c_n^3}, \tag{A5}$$

where $\hat{N}^2$ is a characteristic constant bulk value of N^2. The results above rest on the assumption $|\alpha_n|/k_n \ll 1$. Finally, the baroclinic Rossby radius a_n and the small frictionally induced wave number l_n in the y direction are given by

$$a_n = \frac{\omega}{k_n f} = \frac{c_n}{f}, \quad l_n = \frac{f\alpha_n}{\omega}. \tag{A6}$$

Details of this analysis are found in *Weber and Ghaffari* [2014]. The only difference is that we here for the product $\nu_T N^2$ in the friction terms assume that ν_T is constant, and that N^2 takes on the constant value $\hat{N}^2$. In principle, the displacement amplitudes $A_1, A_2, A_3 \ldots$ in (A4) must be determined from field observations, or analytical/numerical models runs with appropriate forcing.

Acknowledgment
This paper does not contain or use any data. Financial support from the Research Council of Norway through the grant 233901 (experiments on waves in oil and ice) is gratefully acknowledged.

References

Csanady, G. T. (1972), Response of large stratified lakes to wind, *J. Phys. Oceanogr.*, *2*, 3–13.
Farmer, D. M., and J. D. Smith (1980), Tidal interaction of stratified flow with a sill in Knight Inlet, *Deep Sea Res., Part I*, *27*, 239–254.
Gill, A. E., and A. J. Clarke (1974), Wind-induced upwelling, coastal currents and sea-level changes, *Deep Sea Res.*, *21*, 325–345.
Grimshaw, R., and K. Helfrich (2012), The effect of rotation on internal solitary waves, *IMA J. Appl. Math.*, *77*, 326–339.
Kowalik, Z., A. Marchenko, D. Brazhnikov, and N. Marchenko (2015), Tidal currents in the western Svalbard Fjords, *Oceanologia*, *57*, 318–327.
Levine, M. D. (1990), Internal waves under the Arctic pack ice during the Arctic Internal Wave Experiment: The coherence structure, *J. Geophys. Res.*, *95*, 7347–7357.
Lighthill, M. J. (1969), Dynamic response of the Indian Ocean to onset of the Southwest Monsoon, *Philos. Trans. R. Soc. London A*, *265*, 45–92.
Longuet-Higgins, M. S. (1953), Mass transport in water waves, *Philos. Trans. R. Soc. London A*, *245*, 535–581.
Morozov, E. G., and S. V. Pisarev (2002), Internal tides at the Arctic latitudes (numerical experiments), *Oceanology*, *42*, 153–161.
Morozov, E. G., and S. V. Pisarev (2003), Internal tidal waves in the Barents Sea, *Dokl. Earth Sci.*, *393*, 1124–1126.
Morozov, E. G., G. Parrilla-Barrera, M. G. Velarde, and A. D. Scherbinin (2003), The straits of Gibraltar and Kara Gates: A comparison of internal tides, *Oceanol. Acta*, *26*, 231–241.
Morozov, E. G., V. T. Paka, and V. V. Bakhanov (2008), Strong internal tides in the Kara Gates Strait, *Geophys Res. Lett.*, *35*, L16603, doi: 10.1029/2008GL033804.
Ou, H. W., and J. R. Bennett (1979), A theory of the mean flow driven by long internal wave in a rotating basin, with application to Lake Kinneret, *J. Phys. Oceanogr.*, *9*, 1112–1125.
Skarđhamar J., and H. Svendsen (2010), Short-term hydrographic variability in a stratified Arctic fjord, in *Fjord Systems and Archives*, edited by J. A. Howe et al., 344, pp. 51–60, Geological Society, Special Publications, London.
Stokes G. G. (1847), On the theory of oscillatory waves, *Trans. Cam. Phil. Soc.*, *8*, 441–455.
Støylen, E., and J. E. H. Weber (2010), Mass transport induced by internal Kelvin waves beneath shore-fast ice, *J. Geophys. Res.*, *115*, C03022, doi:10.1029/2009JC005298.
Støylen, E., and I. Fer (2014), Tidally induced internal motion in an Arctic fjord, *Nonlinear Processes Geophys.*, *21*, 87–100.
Vlasenko, V., N. Stashchuk, and K. Hutter (2005), *Baroclinic Tides: Theoretical Modeling and Observational Evidence*, Cambridge Univ. Press, Cambridge, U. K.
Weber, J. E. H., and P. Ghaffari (2014), Mass transport in internal coastal Kelvin waves, *Eur. J. Mech. B*, *47*, 151–157.
Weber, J. E. H., K. H. Christensen, and G. Broström (2014), Stokes drift in internal equatorial Kelvin waves; continuous stratification versus two-layer models, *J. Phys. Oceanogr.*, *44*, 591–599.
Wunsch, C. (1973), On the mean drift in large lakes, *Limnol. Oceanogr.*, *18*, 793–795.